

# Structural and optical characterization of ZnO thin films deposited by sol-gel method

A. SINGH<sup>a,b</sup>, A. KUMAR<sup>b</sup>, N. SURI<sup>a\*</sup>, S. KUMAR<sup>c</sup>, M. KUMAR<sup>b</sup>, P. K. KHANNA<sup>a</sup>, D. KUMAR<sup>b</sup>

<sup>a</sup>Hybrid Microcircuit Group, Central Electronics Engineering Research Institute (CEERI)/ Council of Scientific and Industrial Research (CSIR), Pilani-333031 (Rajasthan) India

<sup>b</sup>Electronic Science Department, Kurukshetra University, Kurukshetra

<sup>c</sup>Nano Science and Nano Technology Unit, Indian Institute of Technology, Kanpur

Zinc oxide is a promising semiconductor material with a variety of applications. Transparent, highly crystalline and crack-free film was deposited on corning glass. A transparent sol of 0.33 mol/l was prepared by dissolving Zinc acetate dihydrate in 2-methoxyethanol using mono-ethanolamine as sol stabilizer. Addition of few drops of water turns the sol immediately into milky gel form. The film was annealed in oxygen environment at 500°C for one hour and characterized by X-ray diffraction, Atomic force microscopy, UV-VIS spectroscopy and Raman spectroscopy. Thickness and roughness was measured by Surface profiler.

(Received March 5, 2009; accepted June 15, 2009)

*Keywords:* Raman spectroscopy, Sol-gel, Zinc oxide.

## 1. Introduction

Zinc oxide is a versatile II-VI compound semiconductor material [1] and has gained wide attention in a short time due its large number of applications and superior physical-chemical properties. This material has been widely used in many kinds of application fields such as transparent electrodes in heat mirrors and solar cells [2], surface acoustic wave devices [3], sensors like – gas, humidity, gluucose etc. [4, 5, 6]. Applications of ZnO are also observed as varistors [7], field effect transistors [8], display devices, lasers [9, 10] with ray of hope in finding usage in spintronics [11]. In all applications it is essential to grow crack free and high quality crystalline base of ZnO for fabrication of useful devices. The deposition of thin film of ZnO has been demonstrated by a number of techniques like RF Sputtering [12], spray-pyrolysis [13], metal organic chemical vapor deposition (MOCVD) [14], molecular beam epitaxy (MBE) [15], chemical vapor deposition (CVD) [16], pulse laser deposition (PLD) [10] etc. Amongst the possible competing techniques the sol-gel method [17] offers many advantages for the deposition of thin film, customizable microstructure, ease to compositional modifications, excellent control of stoichiometry of precursor solution, minimum variables to control the growth of film, simple and inexpensive equipments and the possibility of coating deposition on large area substrates. So the sol-gel is a better technique for studies of a large number of materials with different composition [18].

This paper is focused on the deposition of highly crystalline and crack-free undoped ZnO thin films on Corning glass via sol-gel method. In addition to the

standard characterizations, the Raman spectrum of ZnO thin film deposited by sol-gel method is also presented.

## 2. Experimental details

The sol was prepared using zinc acetate dihydrate  $\{(Zn-OOC-CH_3)_2 \cdot 2H_2O\}$  AR of Himedia Chemicals, India, 2-methoxyethanol ( $CH_3-O-CH_2-CH_2-OH$ ) GR of Loba Chemicals, India and mono-ethanolamine ( $C_2H_7NO$ ) AR of Sd-fine Chemicals, India.

To prepare a 0.33 mol/l concentrated sol, appropriate quantity of zinc acetate dihydrate was dissolved in 30 ml of 2-methoxyethanol at 50°C. 2 ml water was also added so that zinc acetate dihydrate dissolves easily due to increase of ionic properties of solvent. Mono-ethanolamine was added immediately as a sol stabilizer in 2:1 ratio to zinc acetate dihydrate. Solution was filtered by Whatman's GF/C class fiber filters to remove dust and other un-dissolved particles. Then the solution was stirred on a magnetic stirrer at 60°C for one hour. The sol was transparent and stabilized for use at room temperature without any precipitate and change in quality. Viscosity of sol was measured by viscometer and it was found to be  $1.70 \times 10^{-3}$  Pa.S.

Zinc oxide thin film was deposited by sol-gel method by using spin coater. Corning 7059 glass was used as substrate. Substrate was first boiled in trichloroethylene and then cleaned in acetone with the help of ultrasonic cleaner.

The precursor sol was dropped on substrate with a cleaned glass dropper and spun at 2000 rpm for 20 s. In last 5 s during spinning the film was dried by hot air with the help of a drier so as to obtain a uniform and crack-free

film. The reason for this drying during spinning, just before the baking process is to avoid contraction of the film on glass substrate due to surface tension effect. After spin coating the film is baked on a hot plate at 300°C for 5 min in air. Thirty layers were coated continuously with similar route, repeating the process. Then this substrate was annealed in a tube furnace at 500°C for an hour in oxygen environment. The flow chart of deposition process is given in Fig. 1.

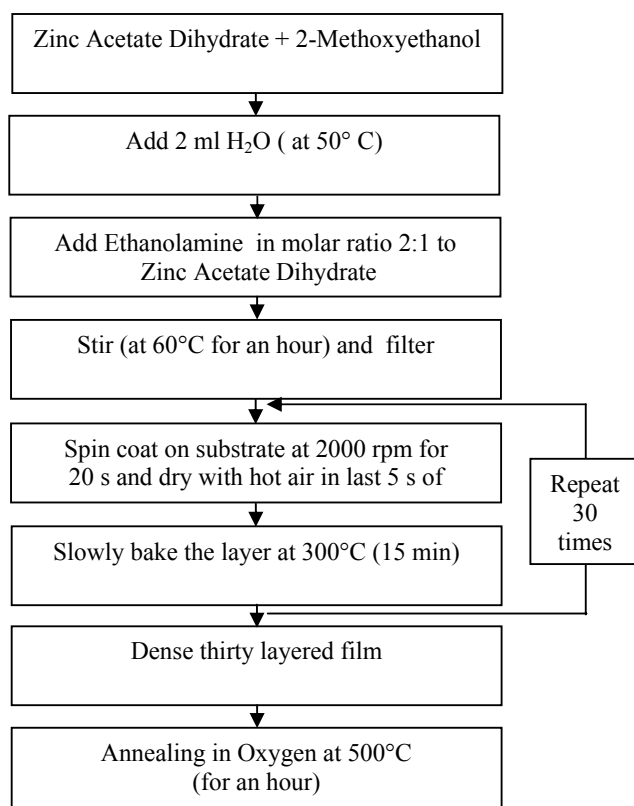


Fig. 1. Flow chart for deposition of ZnO thin film.

The thickness and roughness of the film was measured by Surface profiler. The film was characterized by X-ray diffraction to study the phases and grain size measurement, Atomic force microscopy for topographic studies, UV-VIS spectrometer for transmittance studies and Raman spectroscopy for micro- structural analysis.

### 3. Results and discussion

#### 3.1 Structural characterization

Thickness and surface roughness of the films (with 30 coats) was measured by surface profiler model Ambious XP-1 and the thickness was found to be 117.72 nm so average thickness of each layer was 3.92 nm whereas the roughness of the film was found to be close to 15 nm.

The X-ray diffraction pattern of deposited ZnO thin film is shown in Fig. 2. The X-ray diffraction was obtained by XPERT-PRO Gonio-meter PW3050/60. The pattern shows well defined and sharp peak (observed at 34.44° ( $2\theta$ ) angle) with high intensity which indicates c-axis oriented crystalinity in (002) direction. The relative percentage intensity of all other peaks corresponding to other crystal planes is very low.

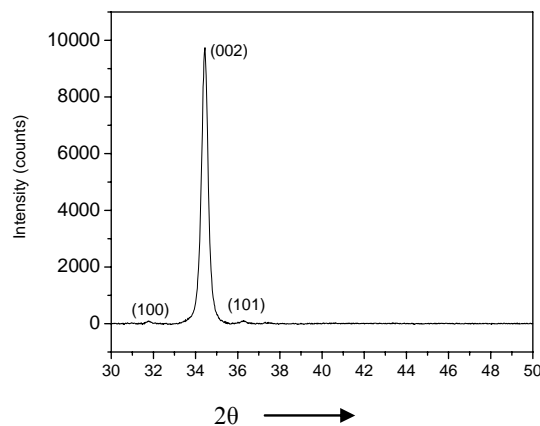


Fig. 2. XRD of ZnO thin film.

In the formation of thin film, crystalinity is disturbed mostly due to oxygen vacancies and interstitial zinc atoms; which is a crystal defect. The film was annealed in the presence of oxygen gas which decrease the defects due to oxygen vacancies hence improves the crystalinity. The lattice constants calculated from the data are  $a = 3.2209 \text{ \AA}$ ,  $c = 5.2075 \text{ \AA}$  respectively. The d-values for the diffraction peaks are in good agreement with standard data book. This shows that the deposited ZnO thin film has a hexagonal wurtzite crystal structure. Grain size is calculated by Scherrer formula from XRD spectra and it is found to be 62.23 nm. AFM image of ZnO thin film is shown in Fig. 3.

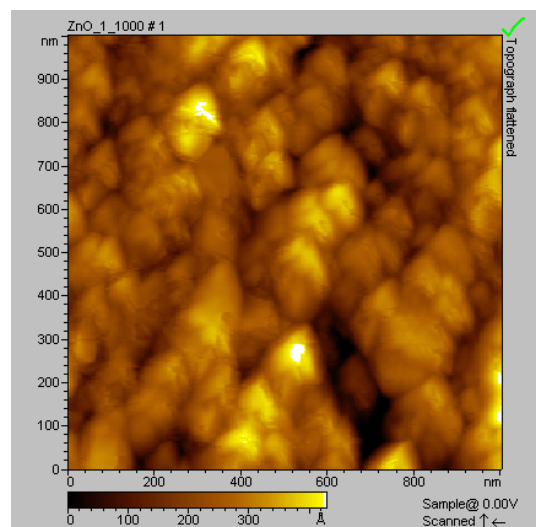


Fig. 3. AFM image of ZnO thin film.

### 3.2 Optical characterization

Fig. 4 depicts the transmission spectra of ZnO thin film on corning glass measured by Shimadzu double beam double monochromatic spectrophotometer (UV#2500). Band gap  $E_g$  of deposited ZnO thin film was calculated by extrapolating the linear portion of transmission spectra. There is a sharp decrease in intensity of transmitted light around 385 nm wavelengths due to band edge absorption. Direct band gap calculated from transmission spectra is 3.22 eV, which is in good agreement with standard data for ZnO.

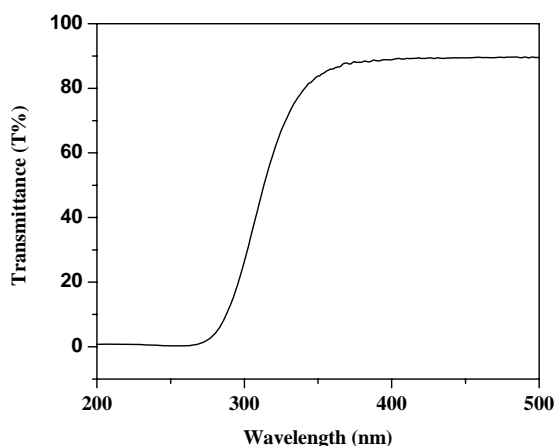


Fig. 4. Transmission spectra of ZnO thin film

### 3.3 Raman characterization

Wurtzite ZnO belongs to space group  $C_{6v}^4$  with two units per primitive cell. The optical phonons symmetries at the  $\Gamma$  point of Brillouin zone can describe by the relation  $\Gamma_{opt} = 1A_1 + 2B_1 + 1E_1 + 2E_2$

Table 1. The comparison of measured Raman shift to the already reported Raman frequencies for ZnO samples.

Symmetry	Measured Wavenumber (thin film) $cm^{-1}$	Ref [19] Experimental (bulk) $cm^{-1}$	Ref [20] Theoretical (bulk) $cm^{-1}$	Ref [21] Experimental (nanowire) $cm^{-1}$
$A_1$	324			331
$A_1(TO)$	385	379	386	383
$E_1(TO)$	408	410	407	410
$E_2$ (high)	437	439	433	438
$A_1$ (LO)	478	574	548	540
$E_1$ (LO)	581	591	628	584

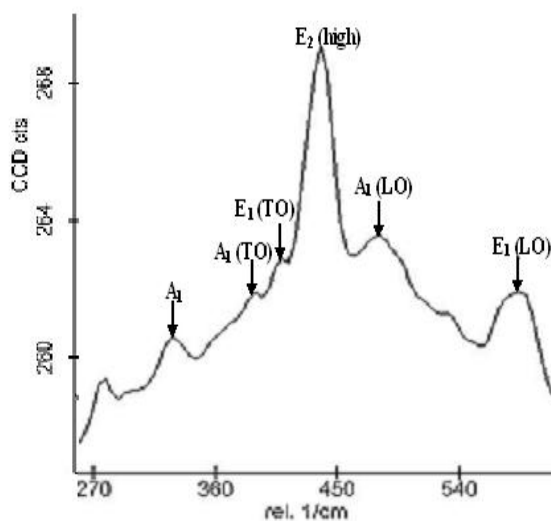


Fig. 5. Raman spectra of ZnO thin film

In the above mentioned relation  $A_1$  and  $E_1$  both are Raman and IR active branches, the two nonpolar  $E_2$  branches are Raman active only and  $B_1$  branches are Raman and IR inactive. The measured Raman spectrum for deposited ZnO thin film is shown in Fig. 5. The film was activated by monochromatic laser of 514 nm wavelengths and a comparison of measured Raman frequencies to the already reported Raman frequencies for bulk, nanowire samples and theoretical data [19-21] is shown in Table 1. Twelve vibrational modes exist in ZnO unit cell – one longitudinal acoustic (LA), two transverse-acoustic (TA), three longitudinal-optical (LO), and six transverse optical (TO).  $A_1$  and  $E_1$  symmetries are polar and split into LO and TO components with different frequencies. One  $E_2$  (high) peak which is corresponding to vibration of oxygen atoms observed at  $437\text{ cm}^{-1}$  is similar to bulk and theoretical data.  $E_2$  (low) peak corresponding to vibration of Zn atoms is not clearly observed in our measurements. The peaks at  $385\text{ cm}^{-1}$  and  $478\text{ cm}^{-1}$  are corresponding to  $A_1$  (TO) and  $A_1$  (LO) respectively. The peaks observed at  $408\text{ cm}^{-1}$  for  $E_1$  (TO) and peak at  $581\text{ cm}^{-1}$  is corresponding to  $E_1$  (LO). The peak ( $A_1$ ) measured at  $324\text{ cm}^{-1}$  is related to multiple phonons scattering process.

## 4. Conclusions

Uniform and highly c-axis oriented nano-crystalline ZnO thin films were deposited on corning glass substrate via sol-gel route and grain size was observed in nanometer range.

The ZnO thin films characterized by XRD show hexagonal wurtzite crystal structure and UV-VIS spectrophotometer results show sharp absorption of electromagnetic waves with wavelength more than 385 nm. There was not much difference found in Raman

frequencies observed in deposited thin film with respect to bulk ZnO sample and theoretical data, although large red shifts were observed in LO mode frequencies in comparison to bulk sample with  $10\text{cm}^{-1}$  shift for  $E_1$  (LO) and  $96\text{cm}^{-1}$  shift for  $A_1$  (LO).

### Acknowledgements

The authors wish to thank all the members of the Hybrid microcircuits group for their support and to the Director CEERI for his encouragement and permission to publish the results.

### References

- [1] A. Onodera, N. Tamaki, Y. Kawamura, T. Sawada, H. Yamashita, *Jpn. J. Appl. Phys-I*, **35**, 5160 (1996).
- [2] W. J. Jeong, S. K. Kim, G. C. Park, *Thin Solid Films*, **180**, 506 (2006).
- [3] G. S. Kino, R. S. Wagers, *J. Appl. Phys*, **44**, 1480 (1973).
- [4] M. Suhea, S. Christoulakis, K. Moschovis, N. Katsarakis, J. Kiriakidis, *Thin Solid Films*, **515**, 551 (2006).
- [5] Z. Bai, C. Xie, M. Hu, S. Zhang, D. Zeng, *Mat. Sci. and Eng.-B*, **149**, 12 (2008).
- [6] J. X. Wang, X. W. Sun, A. Wei, Y. Lei, X. P. Cai, C. M. Li, Z. L. Dong, *Appl. Phys. Lett* **88**, 233106 (2006).
- [7] M. H. Wang, K. A. Hu, B. Y. Zhao, N. F. Zhang, *Matter. Chem. and Phys*, **100**, 142 (2006).
- [8] L. Duan, B. Lin, W. Zhang, S. Zhong, Z. Fua; *Appl. Phys. Lett*, **88**, 232110 (2006).
- [9] A. Jain, P. Sagar, R. M. Mehra, *Solid-State Electronics*, **50**, 1420 (2006).
- [10] R. J. Mendelsberg, J. Kennedy, S. M. Durbin, R. J. Reeves, *Current Appl. Phys*, **8**, 283 (2008).
- [11] Y. Q. Wang, S. L. Yuan, L. Liu, P. Li, X. X. Lan, Z. M. Tian, J. H. He, S. Y. Yin, *J. Magnetism and Magnetic Matter*, **320**, 1423 (2008).
- [12] W. Jun, Y. Yintang, *Matter. Lett*, **62**, 1899 (2008).
- [13] J. H. Lee, B. O. Park, *Matter. Sci Eng.-B*, **106**, 242 (2004).
- [14] O. Pagni, N. N. Somhlahllo, C. Weichsel, A. W. R. Leitch, *Physica-B*, **749**, 376 (2006).
- [15] T. Makino, G. Isoya, Y. Segawa, C. H. Chia, T. Yasuda, M. Kawasaki, A. Ohtomo, K. Tamura, H. Koinuma, *J. Cryst. Growth*, **289**, 214 (2000).
- [16] B. Zhang, X. T. Zhang, H. C. Gong, Z. S. Wu, S. M. Zhou, Z. L. Du, *Phys. Lett.-A*, **372**, 2300 (2008).
- [17] S. O. Brieau, L. H. K. Koh and G. M. Crean, *Thin Solid Films*, **516**, 1391A (2008).
- [18] S. Mridha, D. Basak, *Matter. Res. Bull*, **42**, 875 (2007).
- [19] K. A. Alim, V. A. Fonoberov, M. Shamsa, A. A. Balandin, *J. Appl. Phys*, **97**, 124313 (2005).
- [20] A. Zaoui, W. Sekkal, *Phy. Rev.-B*, **66**, 174106 (2002).
- [21] R. P. Wang, G. Xu, P. Jin, *Phys. Rev.-B*, **69**, 113303 (2004).

\*Corresponding author: surinikhil@redffmail.com